PERKIN 2

Oxo ligand as a reactivity switch in gas-phase ion chemistry of the lanthanides

Hans H. Cornehl, Ralf Wesendrup, Jeremy N. Harvey and Helmut Schwarz *†

Institut für Organische Chemie der Technischen Universität Berlin, Straße des 17. Juni 135, D-10623 Berlin, Germany

The reactions of 'bare' as well as oxo-ligated lanthanide cations with buta-1,3-diene have been systematically investigated. Only those lanthanides with two non-f electrons in their electronic ground state (La, Ce, Gd, Lu) and those which exhibit the lowest excitation energies to such states (Pr, Tb) are able to activate butadiene as 'bare' cations. Dehydrogenation of the organic substrate, loss of ethylene and formation of a butadiene complex (only Lu^+) are the only primary product channels observed, in line with an insertion–elimination mechanism. Upon addition of an oxygen ligand, the lanthanides with the lowest bond energies to oxygen, EuO^+ and YbO^+, preferentially react by transferring the oxygen atom to the hydrocarbon substrate. The reactive Ln^+ becomes inert upon addition of an oxygen ligand, whereas the cationic oxides LnO^+ of the unreactive lanthanides Dy, Ho, Er and Tm activate butadiene. Besides loss of acetylene, the same products as in the reactions of 'bare' Ln^+ are obtained. However, based on a correlation of the reaction rates with the ionisation energies of LnO, a completely different mechanism is proposed for the initial activation step: following an electrophilic attack of LnO^+ on the π-system of the diene, a cationic metalla–oxa cyclohexene is formed as the key intermediate, and this step represents a formal Diels–Alder cycloaddition with LnO^+ acting as a dienophile. The mechanism is further substantiated by additional experimental investigations on LnO^+–isoprene as well as Ln^+–dihydrofuran and Ln^+–tetrahydrofuran systems.

Introduction

Metal centred homogeneous and metal based heterogeneous catalysts play a crucial role in many modern chemical industrial processes and in small-scale preparative syntheses. However, the choice of the appropriate metal, ligands and reaction conditions often remains a matter of trial and error. As a valuable method to study the underlying intrinsic properties of transition metal ions,[1] and thus as a predictive tool for developing and applying new catalysts, ion–molecule reactions in the gas phase have become an area of active research. In this context, the long-neglected lanthanide elements, which are experiencing a renaissance in modern applied catalytic research, have in recent years been the subject of gas-phase investigations.[2] In a systematic study on the gas-phase reactivity of all lanthanide cations Ln^+ towards saturated and unsaturated hydrocarbons it was shown that the ability of Ln^+ to activate C–H or C–C bonds is strongly related to the electronic ground state configuration of the corresponding lanthanide cation. Only those Ln^+ which possess two non-f electrons in their valence shell (La^+, Ce^+ and Gd^+)[3] are able to activate saturated hydrocarbons.[2a,f] The overall reactivity of Ln^+ can be correlated to the excitation energy from the electronic ground state to the lowest state with a $6s^15d^14f^{n-2}$ configuration (n is the number of valence electrons).[2e,f] These findings are rationalised within a qualitative model of an avoided curve crossing of the ground and the corresponding excited state hypersurfaces along the reaction coordinate.

Of course, studying the chemistry of metal ions in the unique experimental environment of a mass spectrometer raises the problem of bridging the gap between these model reactions of isolated species and bulk processes. One first approach to this question is to study the influence of a ligand L on the reactivity of the ML^+ complex, as compared to the 'bare' metal cation M^+. In this respect, oxygenated lanthanide cations should be highly interesting, since lanthanide oxides are among the most abundant compounds of industrial rare-earth production. They are employed in a broad field of applications, *e.g.* in the 'three-way' automobile exhaust converters,[4] superconductors[5] and as butadiene polymerisation catalysts.[6] With respect to gas-phase experiments, the oxygen ligand is expected to change the electronic situation at the metal centre and therefore influence the chemical behaviour of the lanthanides.[2j,7] In this paper we present a comparative study of the gas-phase reactivity of all lanthanide cations Ln^+ (except Pm^+ which does not have any stable isotopes) and oxo-ligated cations LnO^+ towards butadiene. We focus on how the oxo ligand influences the lanthanides' ability to activate C–H and C–C bonds in that particular substrate, and propose a new reaction mechanism for the activation of buta-1,3-diene by LnO^+. In addition, a detailed study of consecutive reaction steps in the HoO^+–butadiene system is included. Finally, a comparison of the oxygen ligand with halide, hydroxy and methoxy ligands is given for neodymium and holmium.

Experimental

The experiments were performed using a Spectrospin-CMS-47X Fourier-transform ion cyclotron resonance mass spectrometer (FTICRMS); the instrument and its operational details have been described elsewhere.[8] Lanthanide ions Ln^+ were generated by laser desorption/laser ionisation in the external ion source by focusing the beam of a Nd:YAG laser (Spectron Systems: $\lambda_{max} = 1064$ nm) onto pure metal pieces (>99%; Tb, Dy, Tm and Yb from Heraeus; La, Ce, Pr, Nd, Sm, Eu, Gd, Ho, Er and Lu from Strem Chemicals). After generation the ions were extracted from the source and transferred *via* a system of electrostatic potentials and lenses into the cylindrical ICR-cell, which is located in the field of a superconducting magnet (Oxford Instruments, max. field strength 7.05 T). Ligated Ln cations LnL^+ and LnL_2^+ ($L = O, OH, OCH_3, F, Cl$) were generated by ion–molecule reactions of Ln^+ with an appropriate pulsed-in reactant gas: O_2 (Ln = Ce, Pr, Gd, Tb,

---

† Fax: Int. code + (30)314-21102; E-Mail: schw0531@www.chem.tu-berlin.de

which form a substantial fraction of LnN^+ in the reaction with N_2O) or N_2O (Ln = Nd, Sm, Eu, Dy–Lu) for LnO^+, O_2–C_2H_5OH for $Ln(OH)_2^+$, SF_6 for LnF^+ and LnF_2^+, CH_2Cl_2 for $LnCl^+$ and $LnCl_2^+$, CH_2Cl_2–H_2O (from background) for $(HO)LnCl^+$ and H_3COOCH_3 for $Ln(OCH_3)_2^+$. The pulse lengths were adjusted to obtain maximum yields of the desired LnL^+ and LnL_2^+ ions, respectively (max. pressure *ca.* 5×10^{-6} mbar). The 'bare' or ligated metal ion corresponding to the most abundant isotope of the lanthanide was isolated using FERETS,[9] a computer-controlled ejection protocol which combines frequency sweeps and single-frequency pulses to optimise ejection of all undesired ions by resonant excitation. Prior to any chemical reaction, the isolated ions were thermalised by allowing them to collide with repeatedly pulsed-in argon (max. pressure *ca.* 5×10^{-5} mbar, *ca.* 1000 collisions per ion). Reactants were admitted to the cell *via* a leak valve at a stationary pressure of $(1–15) \times 10^{-8}$ mbar, as measured by a calibrated ion gauge (BALZERS IMG070). Rate constants were determined from the pseudo first-order decay of the reactant ions and are reported as a percentage of the theoretical collision rate determined according to the average dipole orientation theory (k_{ADO})[10] with an estimated error of ±30%. Thorough thermalisation of the ions was evaluated by the reproducibility of the reaction rates as well as the strict first-order behaviour of the kinetics up to >70% conversion of the reactant ion. Molecular compositions of reaction products were identified using high-resolution mass spectra, and consecutive reactions were investigated by MS/MS and double resonance techniques. All functions of the mass spectrometer were controlled by a Bruker Aspect 3000 minicomputer.

Unfortunately, most of the Ln^+ ions (Ln = La, Ce, Pr, Nd, Sm, Gd, Tb, Dy, Ho and Er) undergo fast side reactions with oxygen sources present as contaminants in the background of the machine (*i.e.* mainly H_2O and O_2). In cases where the undesired processes accounted for more than 5% of the products, the overall reaction rates were multiplied by the initial quota of C–H and C–C bond activation to obtain corrected rate constants for these processes. If reactions of interest were not observed, an upper limit for the overall reaction rate is derived from the pressure of the reactant gas, the reaction time and the signal-to-noise ratio. Branching ratios are calculated from the initial slopes of the primary product-ion intensities and are reported with an estimated error of ±10%.

In this paper the reactions of Ln^+ and LnO^+ with buta-1,3-diene are described, a detailed study on further activation steps is given for the example of HoO^+ and a mechanism for the reactions of LnO^+ with butadiene is proposed and discussed on the basis of further experiments. Also, the effects of halide, hydroxy and methoxy ligands as compared to oxygen are discussed in this context.

Results and discussion

Reactions of Ln^+ and LnO^+ with buta-1,3-diene

Three primary pathways are observed in the reactions of 'bare' lanthanide cations Ln^+ with butadiene (see Scheme 1): (*a*) formation of an acetylene complex with concomitant loss of C_2H_4, most likely ethylene, (*b*) dehydrogenation to yield $LnC_4H_4^+$ and (*c*) formation of a stable adduct complex $LnC_4H_6^+$. The corresponding relative reaction rates and branching ratios are listed in Table 1.

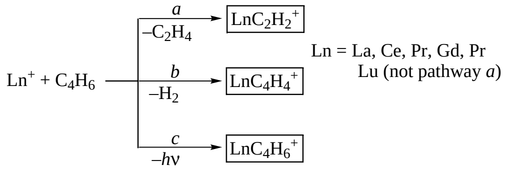

Scheme 1

Table 1 Relative reaction rates (k/k_{ADO}) and branching ratios (in %) for the primary reaction of Ln^+ with buta-1,3-diene. Nd^+–Eu^+ and Dy^+–Yb^+ do not show any reactivity.

Ln^+	k/k_{ADO}	Pathway *a* ($-C_2H_4$)	Pathway *b* ($-H_2$)	Pathway *c* (adduct)
La^+	1.00	65	20	15
Ce^+	1.00	60	30	10
Pr^+	1.00	75	10	15
Gd^+	1.00	70	20	10
Tb^+	0.90	60	20	20
Lu^+	0.10	0	70	30

Only La^+, Ce^+, Pr^+, Gd^+, Tb^+ and Lu^+ are able to mediate C–H or C–C bond activation of butadiene, fully in line with the findings of a recent comparative study on the reactions of Ln^+ with hydrocarbons.[2f] La^+, Ce^+ and Gd^+ possess two non-f valence electrons in their electronic ground state configurations, while Pr^+ and Tb^+ exhibit the lowest excitation energies to a $6s^15d^14f^{n-2}$ configuration within the 4f-row. Their reactions occur close to the collision limit, and the respective branching ratios are identical within experimental error (see Table 1). This observation suggests that the avoided curve-crossing model proposed in ref. 2*f* is also valid for the reactions with butadiene, which points to a reaction mechanism as depicted in Scheme 2:

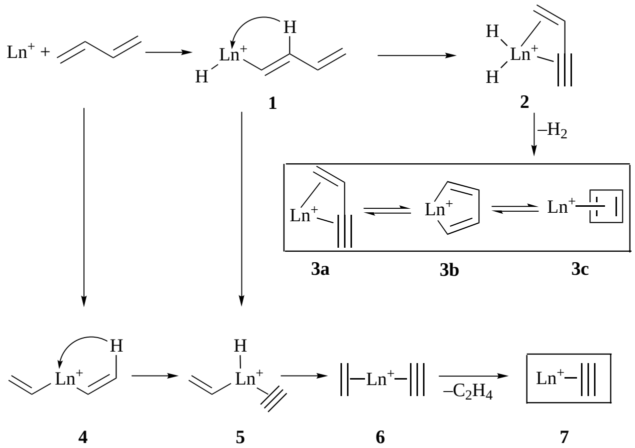

Scheme 2

the metal cation first inserts into a vinylic C–H bond of the hydrocarbon (structure **1**) and subsequent β-H transfer leads to the dihydrovinylacetylene species **2**, which loses a hydrogen molecule to form the product ion $LnC_4H_4^+$. Recent investigations have shown that a precise structural determination for $MC_4H_4^+$ (*e.g.* M = Ru, Rh, W, U) is not possible within the experimental conditions, due to facile interconversion of the isomeric species **3a**–**c** on the $[M^+,C_4,H_4]$ potential energy surface.[11] Alternatively, the initial intermediate **1** may rearrange *via* a β-vinyl shift and reductive elimination of ethylene to yield the acetylene–ethylene complex **6**. Loss of the less strongly bound ethylene then leads to the observed acetylene lanthanide product ion **7**. The exclusive loss of ethylene from **6** suggests that there is a relatively high difference in binding energies as compared to the overall exothermicity of the reaction.[12] However, the significant bias towards C–C activation cannot be fully explained by competition between β-H and β-C shifts from the initially formed **1**, as the latter usually involve higher activation barriers.[13] Thus, in earlier studies, the lanthanide cations were observed to activate hydrocarbons *via* dehydrogenation, instead of by C–C bond cleavage.[2] Therefore, a different mechanism is likely to be operative in the activation of butadiene. We suggest that in the first step the lanthanide cation inserts into the C–C single bond to generate the divinyl complex **4**. Subsequent β-

Table 2 Relative reaction rates (k/k_{ADO}) and branching ratios (in %) for the primary reaction of LnO^+ with butadiene. LaO^+–SmO^+, GdO^+ and TbO^+ do not exhibit any reactivity.

		Reaction Pathways					
Ln^+	k/k_{ADO}	(*a*) ($-C_2H_4$)	(*b*) ($-C_2H_2$)	(*c*) ($-H_2$)	(*d*) (adduct)	(*e*) ($-C_4H_5^{\bullet}$)	(*f*) ($-C_4H_6O$)
Eu^+	1.0	—	—	—	—	40	60
Dy^+	0.01	—	—	20	80	—	—
Ho^+	0.05	—	—	50	50	—	—
Er^+	0.8	50	30	20	—	—	—
Tm^+	1.0	60	20	20	—	—	—
Yb^+	1.0	—	—	—	—	<1	>99
Lu^+	1.0	35	35	—	30	—	—

hydrogen transfer leads to structure **5** which upon rearrangement also yields the bisligated complex **6**.

Obviously, this step is preferred over the C–H insertion to yield **1**. This is at first sight surprising because the bond dissociation energy (E_d) of the inner C–C bond [$E_d(CH_2CH–CHCH_2) = 116.9 \pm 1.8$ kcal mol^{-1}][14] is slightly higher than that of the primary C–H bond in butadiene. The E_d of the latter is not available in the literature, but it should be approximately the same as in ethylene [$E_d(CH_2CH–H) = 111.2 \pm 1.0$ kcal mol^{-1}].[14] This unusually high C–C bond strength is partly due to resonance stabilisation by *ca.* 4 kcal mol^{-1}[15] of the conjugated π-bonds compared with unconjugated systems. However, insertion of an open shell metal centre, here Ln^+, into this bond does not necessarily disrupt the conjugation to yield two isolated double bonds, but may indeed be favoured by resonance interaction of the π-systems with the unoccupied d-orbitals on lanthanum,‡ which would explain the preferential formation of the inserted species **4**, and therefore of the C–C activation product $LnC_2H_2^+$ (**7**).

The behaviour of Lu^+ towards butadiene is somewhat different compared to the other Ln^+ systems above. The reaction rate is one order of magnitude lower ($k/k_{ADO} = 0.10$) and besides formation of a stable adduct complex, only the C–H bond activation (pathway *b*) is brought about, while C–C bond activation is absent. These findings serve as another example for the special position this metal takes among the 4f-elements. A similar observation was made in the reactions of Ln^+ with fluorobenzene,[2h] where Lu^+ also reacts at lower rates and showed a significantly less pronounced tendency to bring about C–C bond activation compared to La^+, Ce^+, Gd^+ and Tb^+.

Upon addition of an oxygen ligand to the lanthanide cations, their behaviour towards buta-1,3-diene changes dramatically, and according to the observed reaction schemes the oxo cations LnO^+ may be classified into four different groups (see Scheme 3). (*i*) Those Ln^+ ions that were able to activate butadiene as 'bare' metal cations (Ln = La, Ce, Pr, Gd, Tb) become completely inert, with the notable exception of Lu^+. (*ii*) The lanthanides from the middle of the first half of the 4f-row, namely Nd and Sm, show no reactivity towards the substrate under investigation either as 'bare' Ln^+ or as diatomic LnO^+ species. (*iii*) The LnO^+ cations from the middle of the second half (DyO^+–TmO^+) reveal a reactivity that is, as far as the neutral products are concerned, comparable to that found for the reactive 'bare' cations. C–H and C–C bond activation processes as well as formation of stable adduct complexes are observed. (*iv*) EuO^+ and YbO^+ follow completely different reaction pathways. Here, transfer of an oxygen atom to the hydrocarbon takes place as the major process. Abstraction of a hydrogen atom from the substrate with concomitant loss of the corresponding neutral organic radical is followed as an alternative pathway. A more detailed description of the latter two groups of LnO^+ is given in the following two paragraphs.

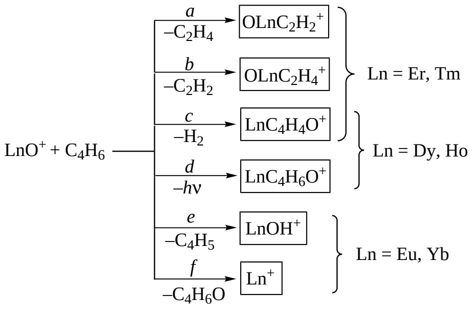

Scheme 3

The relative rates and branching ratios for the reactions of LnO^+ (Ln = Dy–Tm) with buta-1,3-diene (see Table 2 and Scheme 3) vary systematically when going from DyO^+, through HoO^+ and ErO^+, to TmO^+. The reaction of DyO^+ with butadiene occurs at only 1% efficiency, and just a small fraction of the products corresponds to a genuine activation process, *i.e.* expulsion of H_2 from the organic substrate to yield $DyC_4H_4O^+$. HoO^+ reacts in 5% of the collision rate with a branching ratio of 50% towards C–H bond activation. However, neither DyO^+ nor HoO^+ is able to break a C–C bond in butadiene. In contrast, ErO^+ and TmO^+, which react close to the collision limit, preferentially yield C–C bond activation products. As already found for the 'bare' Ln^+, loss of neutral ethylene from butadiene represents the major pathway (*a*; *ca.* 60%), but a substantial fraction of acetylene loss (pathway *b*; *ca.* 20%) is also observed. This behaviour can be rationalised in a structural picture analogous to the one already proposed for Ln^+ (Scheme 2, structure **6**), through formation of an intermediate $OLn^+(C_2H_2)(C_2H_4)$ complex. In contrast to 'bare' Ln^+, the differences in binding energies of acetylene and ethylene are obviously less pronounced for LnO^+ and competing losses of one or the other ligand are observed. Finally, in both cases *ca.* 20% $LnOC_4H_4^+$ is also formed upon loss of a hydrogen molecule (pathway *c*). Notably, neither ErO^+ nor TmO^+ form stable adducts with butadiene (pathway *d*).

The fifth pathway, transfer of the oxygen atom from LnO^+ to butadiene (Scheme 3, pathway *f*), requires a maximum $E_d(Ln^+–O)$ of 119 kcal mol^{-1}, if the thermochemically most stable (C_4H_6O) isomer, methyl vinyl ketone, is formed.[14a] Accordingly, this oxidation (pathway *f*) is only achieved by the weakest bound oxides along the 4f-row, EuO^+ [$E_d(Eu^+–O) = 99 \pm 21$ kcal mol^{-1}] and YbO^+ [$E_d(Yb^+–O) = 90 \pm 9$ kcal mol^{-1}].[17] The weak bond dissociation energies in EuO^+ and YbO^+ point towards a radical-like character of the oxygen ligand rather than a $Ln^+{=}O$ double bond, a phenomenon that has already been analysed in transition-metal oxides, *e.g.* MnO^+.[18] This electronic structure also enables abstraction of a single hydrogen atom from buta-1,3-diene to yield $LnOH^+$ and the neutral radical $C_4H_5^{\bullet}$ which is stabilised by resonance (pathway

---

‡ In fact, extended Hückel calculations for the example of La^+ show that resonance stabilisation of the π-levels in both butadiene and the inserted species $CH_2CH–La^+–CHCH_2$ is of the same order of magnitude.[16]

e), a process that is pursued by EuO^+ at a branching ratio of 40%. In the case of YbO^+ however, pathway *e* is hardly followed (<1%), presumably due to competition from the thermochemically favourable oxidation process (pathway *f*).

Oligomerisation of butadiene by HoO^+

As cationic lanthanide oxides are employed as catalysts for the polymerisation of butadiene, we also investigated the secondary reaction steps for the HoO^+–butadiene system for comparison. Holmium was chosen for several reasons. (*i*) Its cationic oxide is the first along the 4f-row which dehydrogenates butadiene at a rate sufficient for MS^n ($n > 2$) experiments. (*ii*) Holmium is an isotopically pure element, a requirement for high ion intensities since all ions transferred to the ICR cell are available in the experiment and loss of intensity upon isolation of a single isotope is avoided. This point is of crucial importance since several of the experiments described below were carried out at the detection limit of the machine. (*iii*) Holmium is the congener of the second half of the 4f-row to neodymium, which is one of the cheapest lanthanide elements and, therefore, of potential interest for industrial applications. In a series of test experiments, Nd-containing catalysts have shown promising activity in polymerising butadiene.[6]

Scheme 4 summarises the experimental results for the reaction of HoO^+ with butadiene and two subsequent reactions. As described above, HoO^+ reacts at $k/k_{ADO} = 0.05$ to yield the ionic products $HoC_4H_4O^+$ and $HoC_4H_6O^+$ in equal amounts. The dehydrogenation product $HoC_4H_4O^+$ is highly reactive and efficiently dehydrogenates a second molecule of butadiene ($k/k_{ADO} = 1.0$) to give $HoC_8H_8O^+$ as exclusive product. The following reaction of $HoC_8H_8O^+$ is an order of magnitude slower ($k/k_{ADO} = 0.10$). Addition of another C_4H_6 unit to yield $HoC_{12}H_{14}O^+$ (70%), as well as the dehydrogenation product $HoC_{12}H_{12}O^+$ (30%), was observed. The other primary product, $HoC_4H_6O^+$, also reacts faster with butadiene than HoO^+ itself ($k/k_{ADO} = 0.15$), but the effect is less pronounced. Again, addition of butadiene ($HoC_8H_{12}O^+$, 70%) or its dehydrogenation ($HoC_8H_{10}O^+$, 30%) occur as competing pathways. The evaluation of further reaction steps was not possible as sufficient intensities of isolated $HoC_8H_mO^+$ ($m = 10$, 12) or $HoC_{12}H_nO^+$ ($n = 12$, 14) could not be generated.

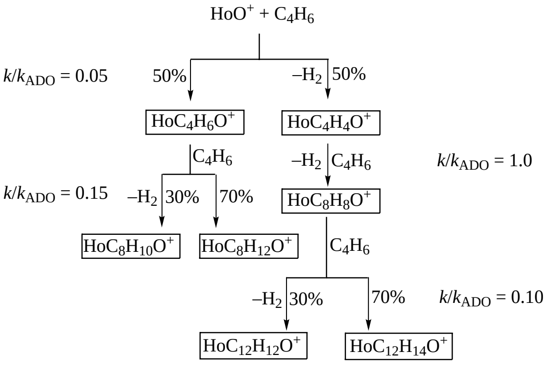

Scheme 4

To gain further information on the structural properties of the intermediates $HoC_4H_nO^+$ ($n = 4$, 6) and $HoC_8H_8O^+$, collision-induced dissociation (CID) with argon as well as ligand-exchange experiments have been performed (Scheme 5). Two decomposition channels are pursued upon collision of kinetically excited $HoC_4H_6O^+$: loss of the intact hydrocarbon moiety to regenerate HoO^+ and loss of C_4H_6O to give 'bare' Ho^+, which indicates that the ion is not necessarily a simple adduct complex between HoO^+ and butadiene. This is supported by the results of the reaction of $HoC_4H_6O^+$ with [1,1,4,4-$^2H_4$]butadiene, where formation of consecutive products according to Scheme 4 as well as stepwise H/D equilibration to give rise to $HoC_4H_{6-n}D_nO^+$ ($n = 1$–4) ions are observed. The thermoneutral ligand displacement of C_4H_6 only occurs in negligible amounts,§ if at all. Although these findings are not unambiguous, they point strongly away from a mere ion–molecule complex of HoO^+ and butadiene. In the CID of the second primary product, $HoC_4H_4O^+$, loss of acetylene to yield $HoC_2H_2O^+$ is found to be a major process, besides the formation of $HoO^+ + C_4H_4$ and $Ho^+ + C_4H_4O$. However, upon reaction of $HoC_4H_4O^+$ with C_2D_2, ligand exchange is not observed which suggests that the C_4-moiety is intact and that loss of C_2H_2 in the CID experiment is due to thermochemical rather than structural reasons. CID of $HoC_8H_8O^+$ also yields HoO^+ (loss of the whole hydrocarbon moiety) and Ho^+ (loss of C_8H_8O). Moreover, a small fraction of H_2O loss is observed, which suggests that the oxygen ligand is not bound only to the metal centre. The absence of hydrocarbon fragments in the CID points towards genuine C–C coupling in the reaction sequence of HoO^+ with two equivalents of butadiene (see Scheme 4).

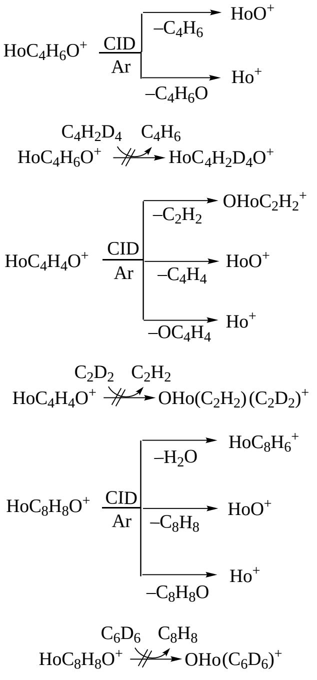

Scheme 5

In view of a potential gas-phase polymerisation, the experimental conditions were changed to probe the limits of subsequent butadiene activation. Instead of reacting isolated HoO^+ with leaked-in butadiene at a static pressure, the substrate was pulsed-in immediately after isolation of the reactant ion. To simulate different reaction times the number of applied pulse cycles was gradually increased up to a maximum substrate pressure of 2×10^{-4} mbar for about 5 s. The overall sequence lasts about 15 s since a pumping delay of 10 s is used to reduce the pressure of butadiene to less than 5×10^{-7} mbar prior to ion detection. Selected spectra obtained for different pulse-lengths are depicted in Fig. 1. At low conversion they mainly contain the products already found in the detailed study of the first reaction steps above, which demonstrates the similarity of both experimental approaches. However, other non-assigned ionic products also appear upon using the pulse values. Their formation can be traced back to reactions of excited precursor ions or to reactions with background contaminants, in particular water, which was also present in the butadiene sample. Despite these difficulties two general conclusions can be drawn for the polymerisation of buta-1,3-diene by HoO^+. (*i*) The reaction

---

§ We cannot exclude that some of the $HoC_4H_2D_4O^+$ ions formed upon reaction with [1,1,4,4-$^2H_4$]butadiene result from ligand displacement, but the relative intensities of the isotopomeric $HoC_4H_{6-n}D_nO^+$ ($n = 1$–4) ions rather suggest that they originate from H/D exchange.

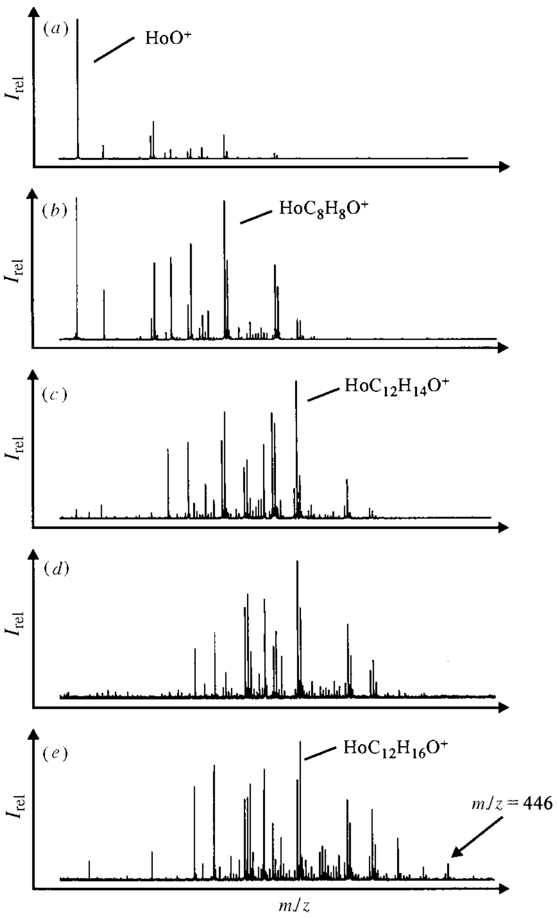

Fig. 1 FTICR mass spectra of the reactions of HoO^+ with pulsed-in buta-1,3-diene. The number of pulse cycles was gradually increased from (*a*) 4 through (*b*) 8, (*c*) 16 and (*d*) 32 up to (*e*) 64.

rate drops with increasing mass of the reactant ions [compare, *e.g.* Fig. 1(*a*)–(*c*) and (*c*)–(*e*)]. A relatively high reactivity of the primary activation products accounts for the dramatic shift of ion signals towards higher masses upon increasing the number of pulse cycles from 4 [Fig. 1(*a*)] to 16 [Fig. 1(*c*)]. In contrast, the subsequent changes [Fig. 1(*c*)–(*e*)] are much less pronounced, as could already be expected from the significant decrease in the reaction rate in going from the second to the third activation step (see Scheme 4). The more butadiene units that are attached to HoO^+, the less reactive the complexes become, which suggests that an active participation of the metal centre is required for the reaction. (*ii*) A maximum number of five butadiene units are consecutively attached to the metal centre corresponding to the peak at $m/z = 446$ in Fig. 1(*e*). Attempts to generate even higher mass products by increasing the number of collisions with butadiene failed, which suggests that the metals ligand sphere is saturated at this stage and further reactions cannot occur.

Mechanistic considerations

Before focusing on the mechanistic details of butadiene activation by LnO^+, some general considerations are indicated. Although examples of Ce^{IV}, Sm^{II}, Eu^{II} and other non-trivalent compounds are known,[19] in the condensed phase most lanthanide compounds are found in the III oxidation state.[20] This general preference for trivalency can be traced back to the fact that states containing more than three non-f valence electrons are energetically unavailable in the lanthanides and that the very compact 4f-electrons belong more to the lanthanides core than to their valence shell. In the LnO^+ species under investigation, the oxidation state III is achieved, so that their electronic valency is completely saturated which should make them particularly inert. Indeed, no reaction is observed for LaO^+ which might be regarded as the prototype for the whole series. 'Perfect pairing'[21] of the $5d^2$ electrons in La^+ (^3F ground state) with the 2p electrons on oxygen (^3P) gives rise to the stable closed-shell $^1\Sigma^+$ ground state and a remarkably high $E_d(La^+–O)$ of 203 ± 7 kcal mol^{-1}.[17,22,23] As is evident from their high bond strengths to oxygen,[17] the early lanthanide oxides CeO^+–NdO^+, as well as GdO^+ and TbO^+, exhibit similar bonding and thus do not activate butadiene either.

In contrast, the significantly weaker Ln^+–O bonds in the late lanthanide oxides as well as in EuO^+ and YbO^+ point towards the growing importance of valence-bond configurations with less strongly coupled bonding pairs.[17] The concomitant higher multi-configurational character of the LnO^+ species opens up new reaction pathways for both thermodynamic and kinetic reasons.[23] In particular, the decreasing $E_d(Ln^+–O)$ value renders the oxidation pathway $LnO^+ + C_4H_6 \longrightarrow Ln^+ + C_4H_6O$ accessible for Ln = Eu, Yb. In parallel, the oxygen ligand gains more radical-like character as it no longer forms a genuine double bond to the lanthanide centre. This radical character is reflected by the abstraction of a hydrogen atom from the hydrocarbon substrate (Ln = Eu, Yb).

However, a more complex explanation is required for the formation of H_2, C_2H_2 and C_2H_4 in the reaction of LnO^+ with butadiene. The metal centred insertion–elimination mechanism derived for the Ln^+–C_4H_6 system cannot be transferred to the LnO^+ cases, as insertion of LnO^+ into a C–H or C–C bond of butadiene would lead to an inaccessibly high oxidation state (V) on the lanthanide centre. Therefore, we propose that the oxygen ligand actively participates in the reaction of LnO^+ with butadiene. Moreover, due to its electronegativity, the oxygen atom increases the effective charge on the metal and consequently the Lewis acidity of the reactant ion. A possible reaction mechanism is depicted in Scheme 6.

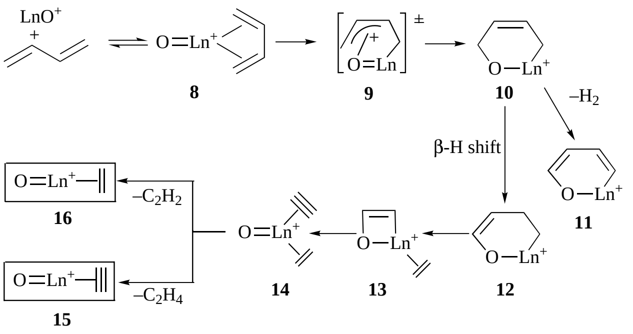

Scheme 6

Starting from the initially formed rovibrationally excited encounter complex **8**, electrophilic attack of the cationic LnO^+ at the π-system of a double bond in butadiene appears plausible.[24] Upon formation of a bond between the lanthanide centre and a terminal carbon atom,[24a] the charge is at least partly transferred to the organic substrate and stabilised due to the proximity of the other π-system in an allylic configuration as well as by interaction with the partial negative charge on oxygen (structure **9**). Subsequent formation of a carbon–oxygen bond to the second terminal carbon atom leads to the metalla–oxa cyclohexene **10**. Dehydrogenation of **10** yields $LnC_4H_4O^+$ for which the cycle **11** represents a reasonable structural suggestion. In a related investigation by Freiser and co-workers, analogous cyclic structures have been proposed for the reductive coupling of ethylene by YNH^+, which resembles LnO^+ as far as the electronic structure is concerned.[25] Alternatively to the loss of hydrogen, **10** may rearrange to **12** which upon β-carbon bond cleavage subsequently leads to the cationic metalla–oxa cyclobutene **13**. Ring opening to the acetylene and ethylene ligated lanthanide oxide **14** followed by loss of either the ethylene or the acetylene ligand from **14** yields the observed $OLn^+C_2H_2$ **15** and $OLn^+C_2H_4$ **16** product ions.

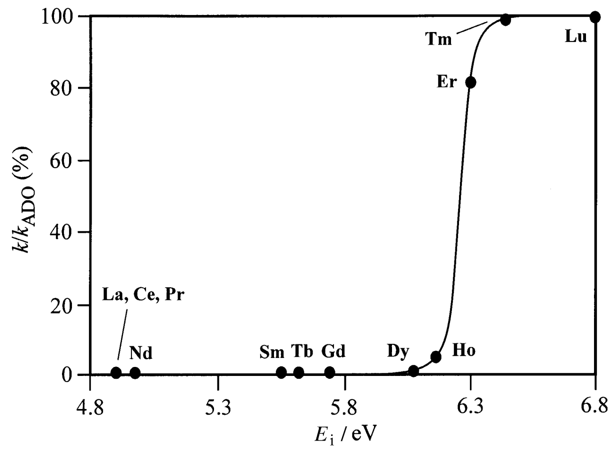

Fig. 2 Plot of rates k relative to k_{ADO} of the reactions of LnO^+ with butadiene *vs.* the ionisation energies of LnO

In the reactions of HoO^+ and TmO^+ with labelled [1,1,4,4-$^2H_4$]butadiene, H/D-equilibration is observed in all ionic products which indicates that the elementary steps leading from **10** to the products are at least in part reversible under the experimental conditions chosen.

While so far the mechanistic scenario has been derived from the reaction products, the reaction efficiencies also support the chosen model. Most interestingly, the relative rate for reaction of LnO^+ with butadiene depends strongly on the ionisation energy of the neutral lanthanide oxide,¶ this correlation is depicted in Fig. 2.|| From the sigmoid dependence of the relative reactivity, it can be concluded that for DyO^+ and HoO^+, the two oxides which represent the 'onset' in LnO^+ reactivity with butadiene, the rate-determining barrier is at or slightly above the entrance channel, whereas for ErO^+ it is already significantly below.

To explain this correlation we refer to solution phase experiments. It has been demonstrated that the reaction rates of organic and organometallic cations with unsaturated hydrocarbons can be correlated with the respective electro- and nucleo-philicity of the reactants according to eqn. (1), where k

$$\log k = s(E + N) \qquad (1)$$

denotes the rate constant and s represents a specific parameter for a certain class of nucleophiles, E and N are parameters which measure the electrophilicity of the cation and the nucleophilicity of the unsaturated substrate.[24] These parameters depend on the experimental conditions and on the properties of the respective reactants. Upon applying eqn. (1) to the gas-phase reactions of the electrophile LnO^+ with the nucleophile buta-1,3-diene in an FTICRMS, the situation becomes much less complicated: s and N are, of course, constant and the relative rates should only depend on the electrophilicity of LnO^+. It appears reasonable that the electrophilicity of LnO^+ depends on their electron affinity and thus on the ionisation energy of the corresponding neutral LnO. This is because the overall similarity of the 4f elements means that the other factors determining $E_i(LnO^+)$ values should remain constant along the 4f row. This assumption is obviously supported by the observed correlation between E_i and k/k_{ADO} values.

Table 3 Ionisation energies of LnO (estimated error ±0.1 eV) according to ref. 26

Ln	E_i(LnO)/eV	Ln	E_i(LnO)/eV
La	4.90	Tb	5.62
Ce	4.90	Dy	6.08
Pr	4.90	Ho	6.17
Nd	4.97	Er	6.30
Sm	5.55	Tm	6.44
Eu	6.48	Yb	6.55
Gd	5.75	Lu	6.79

Table 4 Rates relative to k_{ADO} and branching ratios (in %) for the reactions of LnO^+ with isoprene. For better comparability, lanthanides are listed in the order of increasing E_i(LnO).

Ln^+	k/k_{ADO}	Pathway *a* ($-H_2$)	Pathway *b* ($-C_2H_4$)
Sm^+	<0.001	—	—
Tb^+	0.29	20	80
Gd^+	0.38	25	75
Dy^+	0.46	16	84
Ho^+	0.76	35	65
Er^+	0.92	35	65

According to that model, the reaction rates of the LnO^+–butadiene system also depend on the nucleophilicity of the hydrocarbon. As a consequence, the difference in the ionisation energies of the substrate [E_i(butadiene) = 9.08 eV][14a] and the respective neutral LnO (see Table 3) is of crucial importance for observing a reaction. To check this hypothesis, additional experiments were performed employing the methyl-substituted substrate, isoprene, which has a lower E_i (8.85 eV) and a much higher nucleophilicity[24b] than butadiene. Consequently, some of those LnO^+ which exhibit a value of E_i(LnO) too low to activate buta-1,3-diene should be able to react with isoprene. On the basis of the kinetic results obtained for the LnO^+–butadiene systems, six lanthanides were chosen for this investigation: ErO^+, as a representative of the fast reacting species, DyO^+ and HoO^+ as those cationic oxides which react with butadiene at very low rates, and SmO^+, GdO^+ and TbO^+, which are unreactive towards the latter substrate [E_i(LnO): Sm < Tb < Gd < Dy < Ho < Er; see Table 3].

Two general pathways are observed in the reactions of LnO^+ with isoprene (Scheme 7 and Table 4). (*i*) Single dehydrogenation of isoprene leading to a product ion of composition $LnC_5H_6O^+$ (pathway *a*), which has not been further characterised. (*ii*) Loss of a C_2H_4 molecule giving rise to $LnC_3H_4O^+$, which probably corresponds to a propyne complex of LnO^+ (pathway *b*). As in the reactions with butadiene, LnO^+ preferentially follows the C–C bond activation pathway (pathway *b*) rather than effecting C–H bond activation (pathway *a*). However, in contrast to the butadiene case, loss of ethylene is the only observed C–C bond activation pathway. This finding can be rationalised by analogy to the mechanism proposed in Scheme 6. Starting from methyl-substituted **10**, the double bond is expected to shift to the more substituted 1,2-position of the isoprene fragment. Subsequent cleavage of the inner C^2–C^3 bond results in an $OLn^+(C_3H_4)(C_2H_4)$ complex. Since propyne is more strongly bound to the metal centre than acetylene, the difference in binding energies between both ligands is increased which accounts for the selective loss of ethylene in this case.

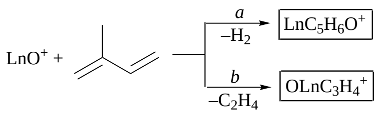

Scheme 7

¶ The revised compilation of ionisation energies for LnO given in ref. 17 is partially based on different experimental sources along the lanthanide row. For the present comparative purpose it seems indicated to refer to the values from the original publication, in which all LnO have been consistently investigated under identical experimental conditions.[26]

|| A qualitative correlation is also found between the reactivity and $E_d(Ln^+–O)$, with the less strongly bound lanthanide oxo cations LnO^+ reacting faster, which is a consequence of the interdependence between the ionisation energy (E_i) and E_d of the lanthanide oxides.

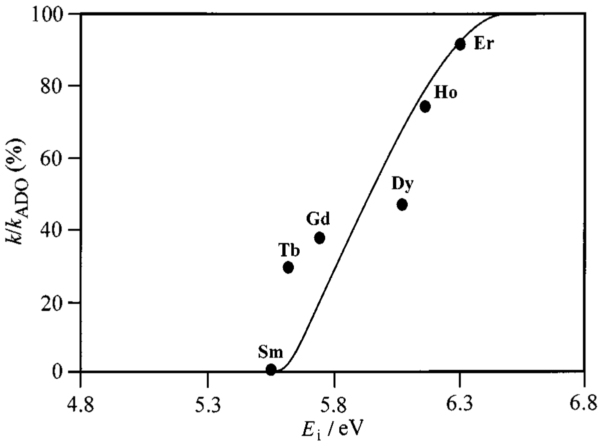

Fig. 3 Plot of rates k relative to k_{ADO} of the reactions of LnO^+ with isoprene *vs.* the ionisation energies of LnO

Since the analogous product distributions indicate that isoprene and buta-1,3-diene react according to the same mechanism, we may now consider the reaction rates. In accordance with the above model, the reaction efficiencies given in Table 4 clearly indicate that the sigmoid curve depicted in Fig. 2 and, in particular, the reactivity onset are shifted towards lower E_i(LnO) values (see Fig. 3). HoO^+ ($k/k_{ADO} = 0.76$) and DyO^+ ($k/K_{ADO} = 0.46$), which only activate buta-1,3-diene very slowly (see above), react readily with isoprene. Even more convincingly, GdO^+ ($k/k_{ADO} = 0.38$) and TbO^+ ($k/k_{ADO} = 0.29$), which are inert towards buta-1,3-diene now exhibit significant reactivity. In line with the higher E_i(GdO) value compared to E_i(TbO), the former ion reacts faster than the latter. Finally, SmO^+, which has the lowest E_i(LnO) value among the six oxides discussed here, is also found to be inert towards isoprene.

The reactivity shift towards lower E_i(LnO) amounts to about 0.4 eV which is more than the difference E_i(buta-1,3-diene) − E_i(isoprene) = 0.23.[14a] This finding is not surprising for two reasons. (*i*) Although the differences in ionisation energies appear to be of crucial importance for the LnO^+–diene systems within the model of an electrophilic attack, the substrates' ionisation energies cannot be regarded as a quantitative measure of their nucleophilicity. (*ii*) The well of the initially formed ion–molecule complex (see Scheme 6, structure **8**) is certainly deeper for isoprene as compared to butadiene. Thus, the energies of the following intermediates and in particular of the rate determining transition structure (Scheme 6, **8**→**10**) are lowered relative to the entrance channel, which also accounts for the observed shift of 0.4 eV. Both effects also are reflected by the decreased slope of the sigmoid curve for the isoprene cases (Fig. 3) as compared to the butadiene cases (Fig. 2). In summary, these findings clearly indicate that the E_i(LnO) values may well serve as a crucial parameter for the height of the rate-determining barrier associated with the observed activation processes.

Formation of the cationic metalla–oxa cyclohexene **10** is a key step in the proposed mechanism of Scheme 6. As it has been shown for $HoC_4H_6O^+$ (previous section), CID and ligand exchange experiments are inconclusive and do not provide unambiguous structural information. In this context, another experimental finding should be emphasised (see first section): only DyO^+ and HoO^+, which slowly react with butadiene, form an ionic product of the composition $LnC_4H_6O^+$ whereas no corresponding products are observed either for the inert LnO^+ ions (Ln = La, Ce, Pr, Nd, Sm, Gd, Tb) or for the ones which react quickly (Ln = Er, Dy).** This observation suggests that the ion $LnC_4H_6O^+$ is not a simple ion–molecule complex **8** which could also be formed from the inert LnO^+, since the efficiencies for collisional and radiative cooling of the adduct should be similar along the lanthanide series. Instead, $LnC_4H_6O^+$ can be considered to be the cyclic intermediate **10**, and its formation is associated with an energetic barrier insurmountable for the inert LnO^+. The fact that C–C bond activation is not observed for DyO^+ and HoO^+ and that $LnC_4H_6O^+$ (Ln = Dy, Ho) is not completely converted to the corresponding C–H activation product $LnC_4H_4O^+$ points towards significant barriers also for these subsequent reaction steps; the one for C–C activation lying above and for C–H activation slightly below the entrance channel. However, as the primary activation barrier involving **9** is lowered for ErO^+ and TmO^+ the subsequent barriers are obviously concomitantly lowered allowing for fast and complete conversion of **10** to C–H and C–C bond activation products.

Table 5 Reaction rates relative to k_{ADO} and branching ratios (in %) of Ln^+ (Ln = Ho, Tm) with dihydrofuran

	2,5-Dihydrofuran		2,3-Dihydrofuran	
	Ho^+	Tm^+	Ho^+	Tm^+
k/k_{ADO}	0.50	0.41	0.27	0.41
Neutrals lost	Branching ratios		Branching ratios	
(*a*) C_2H_4	20	50	15	95
(*b*) C_2H_2	5	15	5	3
(*c*) H_2	10	10	20	2
(*d*) C_4H_6	65	25	60	—

As additional evidence for a cyclic intermediate *en route* to the products, an alternative experimental approach was chosen: 'bare' Ho^+ and Tm^+ cations were reacted with 2,3-dihydrofuran, 2,5-dihydrofuran and tetrahydrofuran. In line with earlier studies on the reactions of transition metal cations with ethers,[27] activation of these substrates is expected to proceed *via* initial insertion of Ln^+ into a C–O bond yielding metalla–oxa cycles similar to structure **10** in Scheme 6. Thus, they serve as model systems to further probe the observed reactivity of LnO^+ with butadiene. Four different pathways are pursued in the reactions of Ln^+ with the two isomeric dihydrofurans (see Scheme 8 and Table 5): (*a*)/(*b*) as in the LnO^+–C_4H_6 reactions, loss of C_2H_4 or C_2H_2 yields $OLn^+C_2H_2$ and $OLn^+C_2H_4$, respectively, which are most probably complexes of LnO^+ with acetylene and ethylene. (*c*) Dehydrogenation leads to $LnC_4H_4O^+$. (*d*) Transfer of an oxygen atom from the substrate to Ln^+ leads to formation of the cationic oxide LnO^+ and the neutral C_4H_6 moiety, which is most probably butadiene, by far the most stable C_4H_6 isomer.

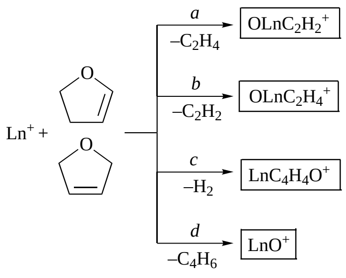

Scheme 8

Ho^+ reacts significantly faster than Tm^+ since, unlike the reactions of LnO^+, the reactions with cyclic ethers are partially driven by formation of the Ln^+–O bond, and this process is *ca.* 25 kcal mol^{-1} more exothermic for Ho^+.[17] Abstraction of an O-atom from 2,5-dihydrofuran to yield buta-1,3-diene requires 101.9 ± 1.2 kcal mol^{-1},[14] thus, formation of HoO^+ is exothermic by at least 19 kcal mol^{-1} which accounts for the major occurrence of the corresponding process in the case of Ho^+ (pathway *d*, 65%). This also means that the Ho^+–2,5-dihydrofuran entrance channel lies at least 19 kcal mol^{-1} above HoO^+–buta-1,3-diene on the $[Ho,C_4,H_6,O]^+$ potential energy surface

---

** EuO^+ and YbO^+ are not taken into account here, since they follow completely different pathways (see above).

Table 6 Reaction rates relative to k_{ADO} and branching ratios (in %) of Ln^+ (Ln = Ho, Tm) with tetrahydrofuran

	Ho^+	Tm^+
k/k_{ADO}	0.47	0.27
Neutrals lost	Branching ratios	
(*a*) $-C_2H_4$	18	45
(*b*) $-2\,H_2$	2	—
(*c*) $-H_2$	15	55
(*d*) $-C_4H_8$	65	—

(PES). Therefore, fully in line with the mechanistic model outlined above, substantial fractions of C–C bond activation products (pathways *a*, 20%; *b*, 5%) are observed for the Ho^+–2,5-dihydrofuran system, whereas they were not formed in the reaction of HoO^+ with butadiene. The results obtained for Tm^+ clearly parallel the Ho^+ case. However, as expected from the lower $E_d(Tm^+–O)$ value compared with $E_d(Ho^+–O)$, the proportion of oxygen transfer (pathway *d*, 25%) is decreased in favour of C–C bond activation (pathways *a*, 50%; *b*, 15%). Dehydrogenation of the substrate occurs with literally identical branching ratios (pathway *c*: Ho, 10%; Tm, 10%).

Unfortunately, the heat of formation of 2,3-dihydrofuran is unknown but it can be estimated to be about 5 kcal mol^{-1} lower than $\Delta_f H°$(2,5-dihydrofuran) by comparison of thermochemical data for related systems.[14] Thus, following the line of argument given for 2,5-dihydrofuran, and assuming that for both dihydrofuran isomers the same critical points of the PES are passed *en route* to the products, the observed reactivity differences between both isomers can be rationalised as follows: the lower relative energy of the entrance channel in the 2,3-dihydrofuran case accounts for the lower reaction rates (k/k_{ADO}: Ho^+, 0.27; Tm^+, 0.07) and in particular for the absence of the oxygen transfer pathway (*d*) in the case of Tm^+. Note that for Ho^+ the ratios of C–C and C–H bond activation remain similar for both isomeric dihydrofurans, whereas a strong bias towards C_2H_4 loss (pathway *a*, 95%) is observed for Tm^+.

Ho^+ reacts at a relative rate of $k/k_{ADO} = 0.47$ with tetrahydrofuran (see Scheme 9 and Table 6), and formation of HoO^+ *via* loss of butene represents the major pathway (*a*, 65%). Fully in line with the C–C bond activation processes observed for the unsaturated systems, one C–C activation channel, loss of C_2H_4 to give rise to $OHo^+C_2H_4$, is followed here (pathway *a*, 18%). Moreover, besides a small fraction of double dehydrogenation (pathway *b*, 2%) single dehydrogenation (pathway *c*, 15%) appears as another major process. As expected, Tm^+ reacts somewhat slower ($k/k_{ADO} = 0.27$) and only pursues pathways *a* (45%) and *c* (55%, see Table 6). Although the Ln^+–tetrahydrofuran systems are not directly related to the other systems discussed before, their consideration is instructive. Formation of $LnC_4H_6O^+$ upon dehydrogenation of this cyclic substrate in conjunction with the observed C–C activation, further supports the assumed cyclic structure of intermediate **10** in Scheme 6.

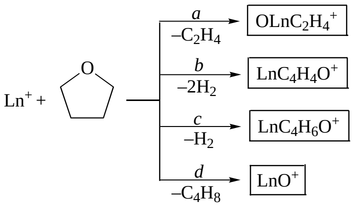

Scheme 9

In a final set of experiments the effect of different ligands on the holmium and neodymium cations was probed. LnL^+ and LnL_2^+ (Ln = Nd, Ho; L = F, Cl, O, OH, OCH_3) were reacted with buta-1,3-diene (Table 7). Like Nd^+ and NdO^+, all other NdL^+ and NdL_2^+ species investigated are unable to activate C_4H_6. The singly ligated species are completely unreactive, whereas the doubly ligated ones undergo very slow formation of adduct complexes. The same is true for Ho^+, HoL^+ and HoL_2^+ with the sole exception being that HoO^+ slowly activates butadiene (see above). Apparently, raising the effective charge on the metal centre as induced by the presence of one or two electronegative ligands is not of primary importance. Nor does the presence of oxygen containing ligands (OH, OCH_3) affect the lanthanide's inertness. The unique influence of a single oxo ligand again indicates an active participation of oxygen within the activation process, *e.g.* by forming $Ln^+–O–R$ (R = hydrocarbon) bonds, which is not possible for the other ligands under investigation.

Table 7 Reaction rates relative to k_{ADO} for the reaction of LnL^+ and LnL_2^+ with buta-1,3-diene

	Neodymium	Holmium
Ln^+	*a*	*a*
LnO^+	*a*	0.05 (adduct/$-H_2$)
LnF^+	*a*	*a*
$LnCl^+$	*a*	*a*
LnF_2^+	0.01 (adduct)	0.02 (adduct)
$LnCl_2^+$	0.02 (adduct)	0.02 (adduct)
$Ln(OH)_2^+$	0.01 (adduct)	0.01 (adduct)
Ln(OH)Cl	0.01 (adduct)	0.02 (adduct)
$Ln(OCH_3)_2^+$	0.02 (adduct)	0.03 (adduct)

[a] No reaction observed ($k/k_{ADO} < 0.001$).

Conclusions

The activation of butadiene by LnO^+ proceeds *via* an electrophilic attack of the cation at the π-system of the diene, and it is proposed that a metalla–oxa cycle **10** acts as a key intermediate *en route* to the products. Its formation formally corresponds to a Diels–Alder type of cyclisation, with LnO^+ acting as dienophile, and represents the rate-determining step in the activation process. The observed reaction rates correlate with E_i(LnO), which reflect the electrophilicity of the corresponding lanthanide oxide cations. Note that the formal [4 + 2] cycloaddition requires formation of a genuine bond between the substrate and oxygen, which explains why reactivity is observed only with this particular ligand.

The gas-phase reactivity of 'bare' lanthanide monocations is dominated by reaction pathways involving oxidative insertion into C–C and C–H bonds. This requires a formal increase in the oxidation level from I to III. Since most condensed-phase lanthanide derivatives occur in the III oxidation state, this type of reactivity cannot be expected to be general, and a more representative gas phase model is represented by the monoxide cations, in which the metal has the III oxidation state. In the present study, we have shown that the addition of an oxygen ligand to the reactive bare lanthanide cations completely suppresses their reactivity, in line with the stable oxidation state III on the metal. However, some of the unreactive lanthanide ions display reactivity with butadiene, following a novel pathway involving electrophilic addition to the carbon skeleton. This reactivity is in much closer agreement with the known condensed-phase properties of lanthanide derivatives.

Acknowledgements

The authors thank the Deutsche Forschungsgemeinschaft, the Fonds der Chemischen Industrie and the Bundesministerium für Bildung, Technologie und Forschung for financial support. J. N. H. thanks the Alexander von Humboldt-Stiftung for a research scholarship. Helpful discussions with Professor Dr Sason Shaik (Hebrew University, Jerusalem, Israel), Professor Dr Antonio Pires de Matos, Dr Joaquím Marçalo (Instituto Technológico e Nuclear, Sacavém, Portugal) and Dr Detlef Schröder (TU Berlin) are gratefully acknowledged.

References

1 Recent reviews: (*a*) P. B. Armentrout, *Ann. Rev. Phys. Chem.*, 1990, **41**, 313; (*b*) J. A. Martinho Simões and J. L. Beauchamp, *Chem. Rev.*, 1990, **90**, 629; (*c*) K. Eller and H. Schwarz, *Chem. Rev.*, 1991, **91**, 1121; (*d*) K. Eller, *Coord. Chem. Rev.*, 1993, **123**, 93; (*e*) J. C. Weisshaar, *Acc. Chem. Res.*, 1993, **26**, 213; (*f*) B. S. Freiser, *J. Mass Spectrom.*, 1996, **31**, 703; (*g*) K. J. Fisher, I. G. Dance and G. D. Willett, *Rapid Commun. Mass Spectrom.*, 1996, **10**, 106.

2 (*a*) J. B. Schilling and J. L. Beauchamp, *J. Am. Chem. Soc.*, 1988, **110**, 15; (*b*) L. S. Sunderlin and P. B. Armentrout, *J. Am. Chem. Soc.*, 1989, **111**, 3845; (*c*) M. Azarro, S. Breton, M. Decouzon and S. Geribaldi, *Int. J. Mass Spectrom. Ion Processes*, 1993, **128**, 1; (*d*) C. Heinemann, D. Schröder and H. Schwarz, *Chem. Ber.*, 1994, **127**, 1807; (*e*) W. W. Yin, A. G. Marshall, J. Marçalo and A. Pires de Matos, *J. Am. Chem. Soc.*, 1994, **116**, 8666; (*f*) H. H. Cornehl, C. Heinemann, D. Schröder and H. Schwarz, *Organometallics*, 1995, **114**, 992; (*g*) J. Marçalo, A. Pires de Matos and W. J. Evans, *Organometallics*, 1996, **15**, 345; (*h*) H. H. Cornehl, G. Hornung and H. Schwarz, *J. Am. Chem. Soc.*, 1996, **118**, 9960; (*i*) J. K. Gibson, *J. Phys. Chem.*, 1996, **100**, 15 688; (*j*) H. H. Cornehl, R. Wesendrup, M. Diefenbach and H. Schwarz, *Chem. Eur. J.*, 1997, **3**, 1083; (*k*) J. N. Harvey, D. Schröder, W. Koch, D. Danovich, S. Shaik and H. Schwarz, *Chem. Phys. Lett.*, 1997, **273**, 164.

3 Atomic data for the lanthanides are given in: W. C. Martin, R. Zalubas and L. Hagan, *Atomic Energy Levels—The Rare Earth Elements*, NSRDS-NBS 60, National Bureau of Standards, Washington DC, 1978.

4 (*a*) F. Bozon-Verduraz and A. Bensalem, *J. Chem. Soc.*, *Faraday Trans.*, 1994, **90**, 653; (*b*) J. Soria, A. Martínez-Arias and J. C. Conesa, *J. Chem. Soc.*, *Faraday Trans.*, 1995, **91**, 1669.

5 (*a*) *Handbook on the Physics and Chemistry of the Rare Earths*, ed. K. A. Gschneider, Jr., and L. Eyring, Elsevier, Amsterdam, 1978 and proceeding volumes until 1995; (*b*) *Industrial Applications of Rare Earth Elements*, ed. K. A. Gschneider, Jr., American Chemical Society, Washington, DC, 1981; (*c*) *Proceedings of the 2nd International Conference on f-Elements*, University of Helsinki, August 1–6, 1994.

6 (*a*) D. J. Wilson, *Polymer*, 1993, **34**, 3504; (*b*) A. Proß, P. Marquart, K.-H. Reichert and T. Knauf, *Angew. Makromol. Chem.*, 1993, **221**, 89; (*c*) D. J. Wilson, *J. Polym. Sci.*, *Polym. Chem.*, 1995, **33**, 2505.

7 C. Heinemann, H. H. Cornehl, D. Schröder, M. Dolg and H. Schwarz, *Inorg. Chem.*, 1996, **35**, 2463.

8 (*a*) K. Eller and H. Schwarz, *Int. J. Mass Spectrom. Ion Processes*, 1989, **93**, 243; (*b*) K. Eller, W. Zummack and H. Schwarz, *J. Am. Chem. Soc.*, 1990, **112**, 621.

9 R. A. Forbes, F. H. Laukien and J. Wronka, *Int. J. Mass Spectrom. Ion Processes*, 1988, **83**, 23.

10 T. Su and M. T. Bowers, *Int. J. Mass Spectrom. Ion Phys.*, 1973, **12**, 347.

11 (*a*) M = U: C. Heinemann, H. H. Cornehl and H. Schwarz, *J. Organomet. Chem.*, 1995, **501**, 201; (*b*) M = W: P. Mourges, A. Ferhati, T. B. McMahon and G. Ohanessian, *Organometallics*, 1997, **16**, 210; (*c*) M = Rh, Ru: R. Wesendrup and H. Schwarz, *Organometallics*, 1997, **16**, 621.

12 For a recent review on that topic, see: P. G. Cooks, J. S. Patrick, T. Kotiaho and S. A. McLuckey, *Mass Spectrom. Rev.*, 1994, **13**, 287, and references therein.

13 See, for example: (*a*) P. E. M. Siegbahn and M. R. A. Blomberg, *J. Am. Chem. Soc.*, 1992, **114**, 10 548; (*b*) C. L. Haynes, E. R. Fisher and P. B. Armentrout, *J. Phys. Chem.*, 1996, **100**, 18 300; (*c*) M. C. Holthausen, Ph.D. Thesis, Technische Universität Berlin, D 83, 1996.

14 (*a*) Standard data are taken from: S. G. Lias, J. F. Liebman, R. D. Levin and S. A. Kafafi, *NIST Standard Reference Database*, *Positive Ion Energetics*, Version 2.01, January 1994; (*b*) the heat of formation of the vinyl radical has been recently revised and the recommended value of 71.6 ± 0.8 kcal mol^{-1} is used here, see: J. Berkowitz, G. B. Ellison and D. Gutman, *J. Phys. Chem.*, 1994, **98**, 2744.

15 (*a*) This value is commonly derived from the barrier for rotation around the inner C–C bond. See, for example: J. March, *Advanced Organic Chemistry*, Wiley, New York, 4th edn., 1992. (*b*) For details, see: B. R. Arnold, V. Balaji and J. Michl, *J. Am. Chem. Soc.*, 1990, **112**, 1808, and references therein.

16 N. Goldberg, Cornell University, Ithaca, personal communication.

17 For a compilation of the available thermochemical data on lanthanide oxides, see: M. C. R. Cockett, L. Nyulászi, T. Veszprémi, T. G. Wright and J. M. Dyke, *J. Electron Spectrosc. Relat. Phenom.*, 1991, **57**, 373.

18 M. F. Ryan, A. Fiedler, D. Schröder and H. Schwarz, *J. Am. Chem. Soc.*, 1995, **117**, 2033.

19 (*a*) For a very recent example of Sm^{II} and Yb^{II} complexes, see: G. B. Deacon, G. D. Fallon, C. M. Forsyth, H. Schumann and R. Weimann, *Chem. Ber.*, 1997, **130**, 409; (*b*) very recently, the first discrete Tm^{II} complex, $[\text{TmI}_2(\text{MeOCH}_2\text{CH}_2\text{OMe})_3]$ has been characterised: M. N. Bochkarev, I. L. Fedushkin, A. A. Fagin, T. V. Petrovskaya, J. W. Ziller, R. N. R. Broomhall-Dillard and W. J. Evans, *Angew. Chem.*, *Int. Ed. Engl.*, 1997, **36**, 133.

20 For example, see: H. Schumann, J. A. Meese-Marktscheffel and L. Esser, *Chem. Rev.*, 1995, **95**, 865.

21 (*a*) A. Fiedler, D. Schröder, S. Shaik and H. Schwarz, *J. Am. Chem. Soc.*, 1994, **116**, 10 734; (*b*) S. Shaik, D. Danovich, A. Fiedler, D. Schröder and H. Schwarz, *Helv. Chim. Acta*, 1995, **78**, 1393.

22 A. Márquez, M. J. Capitán, J. A. Odriozola and J. F. Sanz, *Int. J. Quant. Chem.*, 1994, **52**, 653.

23 A comprehensive overview of electronic structure calculations for molecules containing lanthanide atoms is given in a recent review: M. Dolg and H. Stoll, in *Handbook on the Physics and Chemistry of Rare Earths*, ed. K. A. Gschneider, Jr., and L. Eyring, Elsevier, Amsterdam, 1995, vol. 22.

24 For excellent reviews on solution-phase reactions of cationic organic and organometallic electrophiles with unsaturated hydrocarbon nucleophiles, see: (*a*) H. Mayr, *Angew. Chem.*, *Int. Ed. Engl.*, 1990, **29**, 1371; (*b*) H. Mayr and M. Patz, *Angew. Chem.*, *Int. Ed. Engl.*, 1994, **33**, 938.

25 D. R. A. Ranatunga, Y. D. Hill and B. S. Freiser, *Organometallics*, 1996, **15**, 1242.

26 R. J. Ackermann, E. G. Rauh and R. J. Thorn, *J. Chem. Phys.*, 1976, **65**, 1027, and references therein. These data are also compiled in ref. 14*a*.

27 See, for example: (*a*) R. C. Burnier, G. D. Byrd and B. S. Freiser, *J. Am. Chem. Soc.*, 1981, **103**, 4360; (*b*) M. A. Tolbert and J. L. Beauchamp, *J. Phys. Chem.*, 1986, **90**, 5015.

Paper 7/03084C
Received 6*th May* 1997
Accepted 18*th July* 1997